JOURNAL OF SOLID STATE CHEMISTRY 111, 197–201 (1994)

Subsolidus-Phase Equilibria in the System $MgO–V_2O_5–MoO_3$

V. G. Zubkov and I. A. Leonidov

Institute of Solid State Chemistry, Ural Branch of Academy of Sciences, 91 Pervomayskaia, Yekaterinburg, 620219 Russia

and

K. R. Poeppelmeier[1] and V. L. Kozhevnikov[2]

Chemistry Department of Ipatieff Laboratory, Northwestern University, 2145 Sheridan Road, Evanston, Illinois 60208

Received May 17, 1993; in revised form April 1, 1994; accepted April 6, 1994

IN HONOR OF C. N. R. RAO ON HIS 60TH BIRTHDAY

The phase relations in the system $MgO–V_2O_5–MoO_3$ were studied and the subsolidus region of the phase diagram was constructed. The new compound $Mg_{2.5}VMoO_8$ was discovered on the join of $MgMoO_4–Mg_3V_2O_8$. $Mg_{2.5}VMoO_8$ crystallizes in the orthorhombic space group *Pnma* (No. 62) with cell dimensions $a = 5.0515(1)$ Å, $b = 10.3455(2)$ Å, $c = 17.4683(4)$ Å, and $Z = 6$. The structure is a framework of MoO_4 and VO_4 tetrahedra with linking octahedral and trigonal prismatic MgO_6 groups. The molybdenum and vanadium cations preserve their highest oxidation state, and the electrical neutrality of the crystalline lattice is maintained by partial occupancy of magnesium sites. Simple quasi-binary equilibria were established between $MgMoO_4$ and MoV_2O_8, $V_{2-x}Mo_{2x}O_5$, MgV_2O_6, and $Mg_2V_2O_7$. © 1994 Academic Press, Inc.

INTRODUCTION

Selective heterogeneous oxidation reactions of hydrocarbons are known to be catalyzed by metal oxides. The oxide systems $MgO–V_2O_5$ and $MgO–MoO_3$ have attracted attention in recent years because they have been shown to be active and selective in the oxidation of alkanes. Kung and co-workers (1) have shown that the selective oxidative dehydrogenation of butane to butenes in the system $MgO–V_2O_5$ could be attributed to magnesium orthovanadate $Mg_3V_2O_8$. Selective oxidative dehydrogenation of butane to maleic anhydride has also been reported by Stepanov *et al.* for the $MgO–MoO_3$ system (2), and recently, Murchison has described the oxidation of butane to maleic anhydride over $MgMoO_4$ (3). Therefore, the more complex $MgO–V_2O_5–MoO_3$ system should be interesting as an oxidation catalyst. However, the basic questions on phase compatibility and phase relations in this system are not known. In this report, we present the subsolidus-phase equilibria of the $MgO–V_2O_5–MoO_3$ system. The new compound $Mg_{2.5}VMoO_8$ was identified and its structure was determined. The structure accommodates the transition metal cations in their group's highest oxidation state. Electrical neutrality of the crystalline framework is maintained by the presence of magnesium vacancies.

Based on a review of the literature, the vanadates MgV_2O_6, $Mg_2V_2O_7$, and $Mg_3V_2O_8$ are known in the binary system $MgO–V_2O_5$ (4, 5). Magnesium metavanadate, MgV_2O_6, undergoes a phase transition at 585°C and melts incongruently at 768°C (6). Magnesium pyrovanadate, $Mg_2V_2O_7$, exists in three polymorphic forms: α-$Mg_2V_2O_7$ is stable below 767°C, β-$Mg_2V_2O_7$ exists in the limits 767–918°C, and γ-$Mg_2V_2O^7$ is stable up to 1135°C, where it melts with decomposition. Magnesium orthovanadate, $Mg_3V_2O_8$, is known to be stable in one modification which melts incongruently at 1212°C (7). Two magnesium molybdates are documented reliably in the MgO–MoO3 system (8). Magnesium orthomolybdate, $MgMoO_4$, melts congruently at 1390°C. The molybdate, $MgMo_2O_7$, undergoes a phase transition at 830°C and melts with decomposition at 850°C. The eutectic between $MgMoO_4$ and MgO contains 66 mole% of MgO and melts at 1320°C. The eutectic between MoO_3 and $MgMo_2O_7$ contains 14 mole% of MgO and melts at 745°C. The oxides V_2O_5 and MoO_3 form a solid solution up to 10 mole% MoO_3, at room temperature (9). The intermediate compound MoV_2O_8 was identified (10). The eutectics $V_2O_5–MoV_2O_8$ and $MoV_2O_8–MoO_3$ melt at 644 and 652°C, respectively.

EXPERIMENTAL

Reagent grade oxides MgO, V_2O_5, and MoO_3 (Aldrich) were used as starting reagents. As a preliminary step, the

[1] To whom correspondence should be addressed.

[2] Permanent address: Institute of Solid State Chemistry, Ural Branch of Academy of Sciences, 91 Pervomayskaia, Yekaterinburg, 620219 Russia.

0022-4596/94 $6.00

bordering binary compounds were synthesized according to solid state procedures. The prepared compounds were weighed in desired proportions, milled carefully with addition of ethanol, and then calcined at appropriate temperatures. Owing to the presence of low-temperature eutectics with decreasing magnesia content in the mixtures, a calcination at 600–630°C was implemented for the compositions containing less than 50 mole% of MgO to prevent the formation of liquid phases. The equilibration of these mixtures was performed for 1.5–2 months. The firing temperature was chosen to be 850–900°C for the specimens with larger amounts of magnesia and equilibration was performed for 60–100 hr. The mixtures were ground several times during the calcination procedures. Equilibria were assumed to be established when there were no further changes in the X-ray diffraction patterns. The preliminary X-ray studies were carried out using a Rigaku Geigerflex diffractometer with Cu$K\alpha$ radiation. The data for the structure determination were collected with a STADI-P (STOE, Germany) diffractometer with Cu$K\alpha_1$ radiation using a transmission method and a Ge(111) single-crystal monochomator. The standards were Si (a = 5.43075(5) Å, external) and α-Al_2O_3 (NIST SRM676, internal). The search for an isostructural analog was carried out using SEARCH/MATCH STOE software with the JCPDS-ICDD data base. Structural refinement was carried out using the DBW4.1 program (13), which is a version of the DBW3.2S program adapted for the STOE software. The angle correction for absorption was determined by absorption of the incident beam, $\mu t = \ln (I/I_0)$. Two types of step scans for data acquisition with rotation of sample were used: (i) a scintillation detector, 2θ range = 4–120°, step = 0.02°, FDS = 0.2 mm, acquisition time = 30 min, for preliminary structural refinement; and (ii) large position sensitive detector (PSD), 2θ range = 4–120°, step = 5°, acquistion time = 30 min, for final refinement. PSDs exhibit a noticeable nonlinearity depending on the channel number. However, this nonlinearity in the central part of the detector does not exceed 1%. To avoid the influence of the nonlinearity on the results, the data acquisition was done with a 5° step.

RESULTS AND DISCUSSION

Single-phase materials were not obtained when molybdenum oxides was substituted into magnesium orthovanadate according to the formula $Mg_3V_{2-x}Mo_xO_8$ with x = 0.2 and 0.5. However, a small solubility of molybdenum oxide at 900°C was noticed while substituting it according to the formula $Mg_{3-x}V_{2-2x}Mo_{2x}O_8$. The unit cell parameters of $Mg_{3-x}V_{2-2x}Mo_{2x}O_8$ reacted with small concentrations of molybdenum cations were estimated from the (132), (023), (113) diffraction peaks referenced to those of orthorhombic magnesium orthovanadate. The

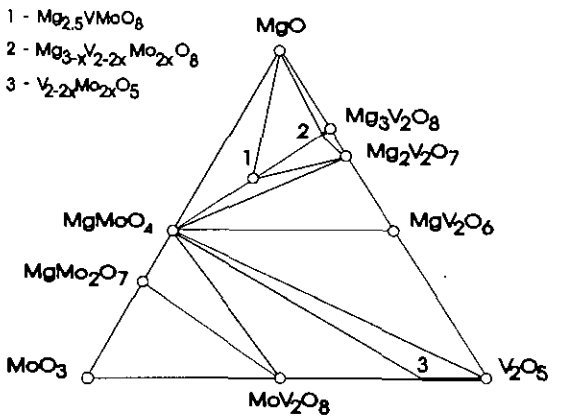

FIG. 1. Subsolidus-phase relations in the triangle MgO–V_2O_5–MoO_3.

lattice, parameters obtained for pure, undoped $Mg_3V_2O_8$ were slightly smaller than the JCPDS-ICDD (Card N37-351) data obtained from a monocrystalline sample. The difference was most likely caused by sample imperfections. From the changes of lattice parameters the solubility limit was estimated to be at $x \sim 0.03$ (11). Systematic triangulation was used to clarify phase constituents at larger molybdena contents (see Fig. 1). Compositions along the lines from the point $MgO : V_2O_5 = 3 : 1$ (orthovanadate) of the binary system MgO–V_2O_5 to the points of the binary system MgO–MoO_3 with ratios of MgO–MoO_3 = 1 : 1, 1.5 : 1, 2 : 1, 3 : 1, and 4 : 1 were investigated. All of these samples showed the presence of an unidentified phase in combination with magnesium orthovanadate ($Mg_3V_2O_8$) or magnesium orthomolybdate ($MgMoO_4$), depending on the composition. The X-ray diffraction patterns of the specimens along the line $Mg_3V_2O_8$–$MgMoO_4$ with overall composition $Mg_{3-x}V_{2-2x}Mo_{2x}O_8$ revealed the existence of two solid phases in equilibrium between the points $0 < x < 0.5$ and $0.5 < x < 1.0$. Additional experiments also showed the equilibrium between MgO and $Mg_{3-x}V_{2-2x}Mo_{2x}O_8$ with x = 0.5. The firing of the oxide mixture $MgO : V_2O_5 : MoO_3 = 6 : 2 : 1$, corresponding to the triangle $Mg_3V_2O_8$–$Mg_2V_2O_7$–$Mg_{2.5}VMoO_8$, gives a three-phase equilibrium between the constituent points. These results demonstrate that the singular point $Mg_{2.5}VMo_8$ corresponds to an individual compound. Moreover, these data also show the existence of equilibria between the compounds $MgMoO_4$–$Mg_{2.5}VMoO_8$, MgO–$Mg_{2.5}VMoO_8$, $Mg_{2.5}VMoO_8$–$Mg_3V_2O_8$, and $Mg_{2.5}VMoO_8$–$Mg_2V_2O_7$.

The octagon which is bordered with the nodes MoO_3, $MgMo_2O_7$, $MgMoO_4$, $Mg_{2.5}VMoO_8$, $Mg_2V_2O_7$, MgV_2O_6, V_2O_5, and MoV_2O_8 and which is arranged from three independent chemical variables (MgO, V_2O_5, MoO_3) contains [(8!/6!2! − 8) − 3] = 17 possible binary equilibria. Recognizing the existence of low-temperature eutectics in this region and the corresponding necessity of using a

low-temperature calcination to avoid the appearance of the liquid phases, an enormous effort would be required to examine all the possible equilibria in a regular fashion. However, empirical experience suggests that pseudobinary equilibria between the binary compounds with equimolar ratio of constituent oxides exist rather often (14). Therefore, the lines ($MgO : MoO_3$ = 1 : 1)–(MgO-V_2O_5 = 1 : 1) and ($MoO_3 : MgO$ = 1 : 1)–($MoO_3 : V_2O_5$ = 1 : 1) were systematically studied. Equimolar ratios of $MgMoO_4$ with MgV_2O_6 and $MgMoO_4$ with MoV_2O_8 were mixed and heated at 600°C for more than 1.5 months with several intermediate grindings. No traces of compounds other than the starting ones were found. Therefore the pseudobinary equilibria $MgMoO_4$–MgV_2O_6 and $MgMoO_4$–MoV_2O_8 exist and no other compounds are present. In analogous long-term calcination experiments, the regions $MgMoO_4$–$Mg_{2.5}VMoO_8$–$Mg_2V_2O_7$–MgV_2O_6, $MgMoO_4$–MgV_2O_6–V_2O_5–MoV_2O_8, and MoV_2O_8–MoO_3–$MgMoO_4$ were resolved without the appearance of new compounds and the simple pseudobinary equilibria $MgMoO_4$–$Mg_2V_2O_7$, $MgMoO_4$–V_2O_5, and $MgMo_2O_7$–MoV_2O_8 were established.

The low-temperature equilibrium $MgMoO_4$–V_2O_5, which substantially determines the subsolidus diagram configuration, required additional evaluation. The mechanical mixture of these components melts at 625°C. As a control experiment, the equimolar mixture of MgV_2O_6 and MoV_2O_8 was reacted at 600°C for nearly 2 months. The X-ray patterns of the starting mixture and of the final product are shown in Fig. 2. The reflections belonging to the phases $MgMoO_4$ and V_2O_5 are evident in the X-ray pattern of the product. Hence, there is a solid state reaction $MgV_2O_6 + MoV_2O_8 \rightarrow MgMoO_4 + 2V_2O_5$ and the equilibrium $MgMoO_4$–V_2O_5 at 600°C was established. Having established the binary equilibria $MgMoO_4$–V_2O_5 and $MgMoO_4$–MgV_2O_8, the line connecting $MgMoO_4$ and the point of the solid solution $V_{2-2x}Mo_{2x}O_5$ can be drawn (see Fig. 1).

The subsolidus equilibria in the triangle MgO–V_2O_5–MoO_3 are shown in Fig. 1. The interesting feature of this diagram is a coexistence of V_2O_5 and $Mg_{2.5}VMoO_8$ with $MgMoO_4$. This suggests that magnesium molybdate $MgMoO_4$, which itself is active in butane oxidation (3), can serve as an active support for vanadium pentoxide V_2O_5 (known to be active in a wide variety of oxidation reactions) or for $Mg_{2.5}VMoO_8$, which has been shown to maintain the good selectivity exhibited by magnesium orthovanadate in the butane oxidation reaction (11).

One important condition for the successful resolution of a structure determination problem on the basis of a powder diffraction pattern is the identification of a structural analog. The two phases $Li_2Ni_2Mo_3O_{12}$ (12) and $NaCo_{2.31}(MoO_4)_3$ (15) were identified as possible models. Both compounds are isostructural and adopt an orthorhombic structure (space group *Pnma*) with the Mo

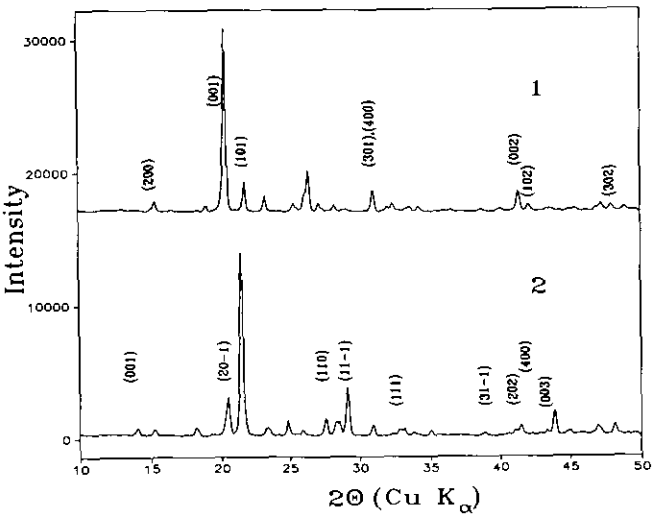

FIG. 2. (1) X-ray pattern of the equimolar mixture MgV_2O_6 + MoV_2O_8 after 2 months of calcination at 600?C in air. Indexes mark V_2O_5; the other peaks belong to $MgMoO_4$. (2) X-ray pattern of the equimolar mechanical mixture MgV_2O_6 + MoV_2O_8. Indexes mark MgV_2O_6; the other peaks belong to MoV_2O_8.

cations in tetrahedral positions (4*c* and 8*d*). The alkali cations reside in trigonal prisms (4*c*, designated M_1 in Fig. 4) and Co or Li and Ni are in octahedral positions (4*c* and 8*d*, designated M_2 and M_3, respectively, in Fig. 4). Based on these observations and taking into account the preference of V^{5+} cations to adopt tetrahedral coordination, one can suppose three variants of the possible cation distribution in $Mg_{2.5}VMoO_8$: (i) Mg_1-8*d*, Mg_2-4*c*, Mg_3-4*c*, $2V_1 + 2Mo_1$-4*c*, $4V_2 + 4Mo_2$-8*d*; (ii) Mg_1-8*d*, Mg_2-4*c*, Mg_3-4*c*, $4V_1$-4*c*, $2V_2 + 6Mo_2$-8*d*; and (iii) Mg_1-8*d*, Mg_2-4*c*, Mg_3-4*c*, $4Mo_1$-4*c*, $6V_2 + 2Mo_2$-8*d*. Comparison of the calculated X-ray patterns for these three models and the experimental data was carried out using the TEO/STOE software. The best correspondence was obtained for model (i). Therefore, the final structural refinement was carried out with this model of the cation distribution. The starting positional parameters for the cations were taken from Ibers and Smith (15). The refinement results are presented in Table 1 and Fig. 3. The atom coordinates are similar to those found in $NaCo_{2.31}(MoO_4)_3$ (15). The *b*–*c* projection of the structure is shown in Fig. 4. The unit cell of the compound $Mg_{2.5}VMoO_8$ comprises six formula units. Therefore, the crystal-chemical formula should be written $Mg_{15}V_6Mo_6O_{48}$.

The refined ion coordinates were used for calculation of the cation–anion distances which are illustrated in Fig. 5. These distances were used to calculate bond valence sums (16). The calculated valence sums for the cations are $Mg_3(+1.80)$, $Mg_2(+2.04)$, $Mg_1(+2.03)$, $V_1 + Mo_1(+5.69)$, and $V_2 + Mo_2(+5.61)$. These values reflect the ionic character of the bonding in $Mg_{2.5}VMoO_8$, i.e., all the cations are in their highest oxidation state (Mg^{2+},

TABLE 1
Crystal and Structure Parameters from Rietveld Refinement for $Mg_{2.5}VMoO_8$

Formula	$Mg_{2.5}VMoO_8$
Molar weight	339.69
Space group (number), Z	*Pnma* (62), 6
Lattice constants a, b, c (Å)	5.0515(1), 10.3455(2), 17.4683(4)
Density d_m, d_x (g/cm³)	3.60(3), 3.71
Number of permitted X-ray reflections	724
Number of the X-ray reflections with intensity $I/I_o > 0.1\%$	250

Atom coordinates and occupancy

Atom	Position	x/a (σx)	y/b (σy)	z/c (σz)	Occupancy
Mg_1	8*d*	0.2577(12)	0.4228(4)	0.4734(2)	1.0
Mg_2	4*c*	0.4025(13)	0.25	0.7568(4)	0.5
Mg_3	4*c*	0.2359(18)	0.25	0.3024(4)	0.45(5)
$V_1 + Mo_1$	4*c*	0.7201(6)	0.25	0.5551(1)	0.25 + 0.25
$V_2 + Mo_2$	8*d*	0.7775(4)	0.4672(6)	0.3415(3)	0.5 + 0.5
O_1	4*c*	0.6469(24)	0.25	0.6558(7)	0.5
O_2	4*c*	0.4587(12)	0.25	0.4971(9)	0.5
O_3	8*d*	0.8485(19)	0.6101(10)	0.2957(10)	1.0
O_4	8*d*	0.9050(15)	0.1172(8)	0.5350(5)	1.0
O_5	8*d*	0.5840(16)	0.5012(10)	0.4274(10)	1.0
O_6	8*d*	0.5596(21)	0.3764(15)	0.2813(10)	1.0
O_7	8*d*	0.0506(10)	0.3880(15)	0.3683(16)	1.0

Note. Standard deviations are shown in parentheses. The reliability factors are pattern $R_p = 3.34\%$, weighted pattern $R_{wp} = 3.36\%$, expected pattern $R_{exp} = 2.78$, Bragg $R_1 = 9.63\%$; overall isotropic temperature factor = 0.21(5) Å².

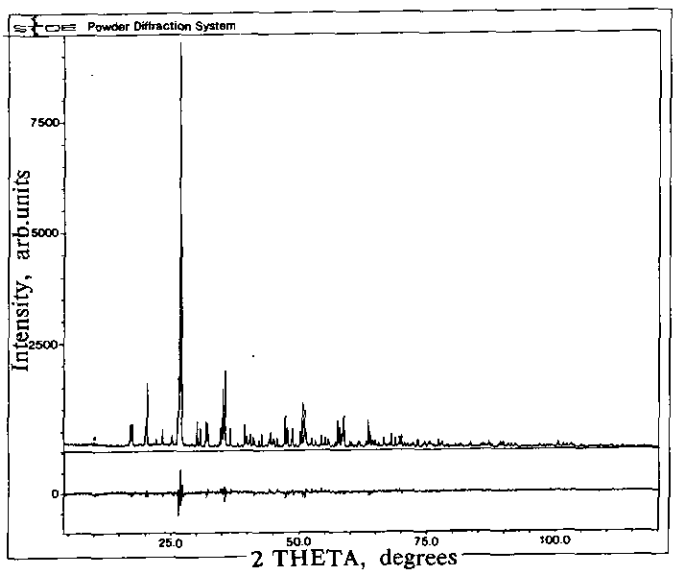

FIG. 3. The observed X-ray pattern and difference plot from Rietveld refinement for $Mg_{2.5}VMoO_8$. *Foil substrate.

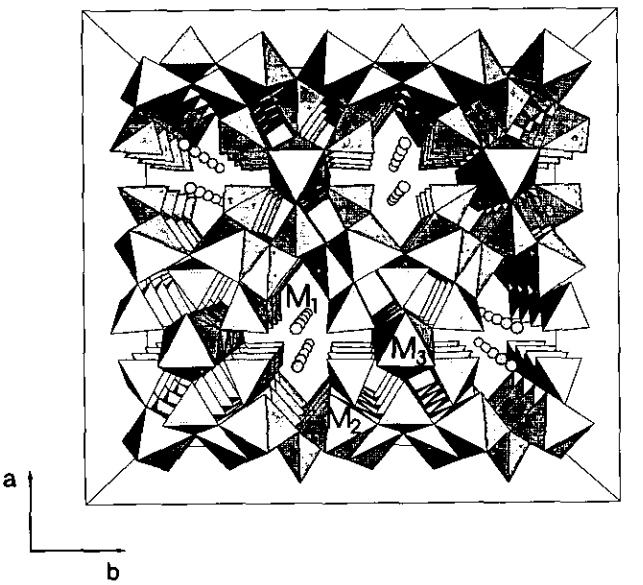

FIG. 4. The b–c projection of the crystal structure of $Mg_{2.5}VMoO_8$. Positions M_1, M_2, and M_3 are shown (see text for their definition).

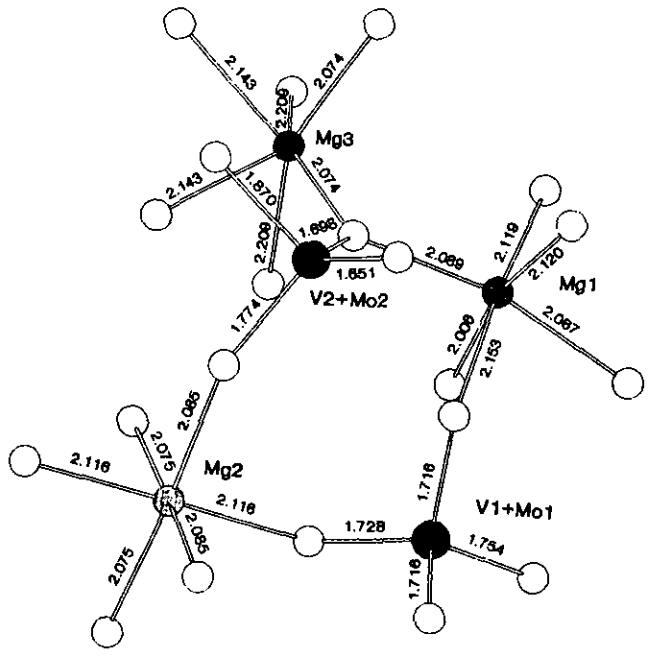

FIG. 5. A fragment of the $Mg_{2.5}VoO_8$ structure. Open circles represent oxygen atoms.

V^{5+}, Mo^{6+}). The slightly decreased value for the Mg_3 ions residing in the trigonal prisms is expected because the prism cavities (designated M_1 in Fig. 4) are too large for the magnesium ion. Therefore, in contrast to $NaCo_{2.31}(MoO_4)_3$, where the charge balance is preserved with trivalent cobalt ions in octahedral coordination (designated M_2 and M_3 in Fig. 4), charge neutrality in $Mg_{2.5}VMoO_8$ is satisfied with magnesium vacancies which are most likely concentrated in the trigonal prismatic (M_1 positions) sites.

A distinct feature of the magnesium orthovanadate, $Mg_3V_2O_8$ (17), compared to the meta- and pyrovanadates, is the isolation of the tetrahedra containing vanadium (5+) between the magnesium containing octahedra. This particular feature of a solid state structure was suggested to be the reason for the high selectivity of $Mg_3V_2O_8$ in the oxidation of butane to butadiene (1). Isolation of the tetrahedra that contain the transition metal cation is preserved in the framework of $Mg_{2.5}VMoO_8$. However, this structure contains three inequivalent six-coordinate positions, which suggests that a wider range of isomorphous substitutions is possible compared to magnesium orthovanadate. Thus, for example, the new compounds $Mg_2Mn_{0.5}VMoO_8$ and $Mg_2Li_{0.25}Fe_{0.25}VMoO_8$ exhibit X-ray patterns similar to that of $Mg_{2.5}VMoO_8$, and compared with almost colorless $Mg_{2.5}VMoO_8$ they are colored.

CONCLUSION

Phase relations of the system $MgO–V_2O_5–MoO_3$ were studied in the subsolidus region and quasi-binary equilibria were established between MoV_2O_8, $V_{2-2x}Mo_{2x}O_5$, MgV_2O_6, $Mg_2V_2O_7$, and $MgMoO_4$. The new compound $Mg_{2.5}VMoO_8$ was found on the quasi-binary line $MgMoO_4–Mg_3V_2O_8$, and as observed with magnesium orthovanadate, $Mg_3V_2O_8$, isolation of the transition metal in tetrahedral MO_4 groups occurs. The vanadium and molybdenum cations have been shown to exist in the +5, +6 oxidation state, respectively, with charge neutrality satisfied by partial occupancy of the magnesium sublattice. Isomorphous substitution of alkali and transition metals on the magnesium sites has been observed.

ACKNOWLEDGEMENT

The authors acknowledge an Extramural Research Award (EMRA) from BP America, Inc., for support of this research.

REFERENCES

1. M. A. Chaar, D. Patel, M. C. Kung, and H. H, Kung, *J. Catal.* **105,** 483 (1987).
2. G. A. Stepanov, A. L. Tsailingol'd, V. A. Levin, and F. S. Pilipenko, *Stud. Surf. Sci. Catal. B* **7,** 1293 (1981).
3. C. Murchison, Report delivered at Catalysis Club of Chicago, Nov. 9, 1992; S.-C. Chang, M. A. Lengers, and M. R. Bare, *J. Phys. Chem.* **96,** 10358 (1992).
4. E. I. Speranskaia, *Trans. AS USSR Inorg. Mater.* **7,** 1809 (1971).
5. R. Wolast and A. Tazait, *Silic. Ind.* **34,** 37 (1969).
6. P. Kohlmuller and T. Perrand, *Bull. Soc. Chim. Fr.* **3,** 642 (1964).
7. A. A. Fotiev, B. V. Slobodin, and M. Ya. Khodos, "Vanadates: Composition, Structure, Properties." Science Moscow, 1988.
8. V. M. Zhukovski, Dissertation, Ural State University, Sverdlovsk, 1974.
9. L. Stanescu, E. Indrea, I. Ardelean, M. Coldea, I. Bratu, and D. Stanescu, *Rev. Roum. Phys.* **21,** 939 (1976).
10. A. Magneli and B. Blomberg, *Acta Chem. Scand.* **5,** 585 (1951).
11. W. D. Harding, H. H. Kung, V. L. Kozhevnikov, and K. R. Poeppelmeier, *J. Catal.* **144,** 597 (1993).
12. A. Ozima, M. Sato, and T. Zoltai, *Acta Crystallogr., Sect. B* **33,** 109 (1989).
13. D. Wiles, a. Sakthevel, and R. Young, "Rietveld Analysis Program—Version DBWS-9006." Georgia Institute of Technology, 1990; S. A. Howard, "A Program for the Rietveld Analysis of X-Ray and Neutron Powder Diffraction Patterns: DBW 4.1." University of Missouri-Rolla, 1989.
14. "Phase Diagrams for Ceramics." Edition of American Ceramic Society, 1964–1984.
15. J. A. Ibers and G. W. Smith, *Acta Crystallogr.* **17,** 1990 (1964).
16. I. D. Brown and D. Altermatt, *Acta Crystallogr., Sect. B* **41,** 244 (1985).